Supplementary Material

Evangelos E. Pompodakis[*], Andreas I. Chrysochos[**], Arif Ahmed[†], Minas C. Alexiadis[‡]
[*‡]Department of Electrical and Computer Engineering, Aristotle University of Thessaloniki, Greece
[**]R&D Department, Hellenic Cables, Greece
[†]TUMCREATE, 1 CREATE Way, #10-02 CREATE Tower, Singapore 138602
Email: [*]bobodakis@hotmail.com, [**]achrysochos@hellenic-cables.com, [†]arif.ahmed@tum-create.edu.sg, [‡]minalex@auth.com

I. Additional Validation Results of the Proposed TEE Circuit Under Extreme Loading Conditions

To further validate our model, we present here the results of two additional simulations under extreme current loading conditions for *Installation 1* (see Fig. 3 of manuscript). Although these loading conditions exceed the thermal limit of the cables and are not realistic, they are applied only to further test the accuracy of the TEE model proposed in Section III of the manuscript.

The loading conditions for the two examined cases are quoted in Tables S1-S2, below, while the responses of the conductor temperatures are depicted in Figs. S1-S2. As shown, the conductor temperature responses of TEE circuit of Fig. 2 of the manuscript (calculated in MATLAB) are in full agreement with those of FEM software, in all examined cases, confirming the accuracy of our model even under extreme loading conditions. More specifically, the maximum deviation observed between the TEE and the FEM is 2 °C for phase b at the 3rd hour of Fig. S2, which corresponds to a deviation of only 0.8%. Similar tests were performed also for the other installations, although they are not depicted here.

TABLE S1
Conductor Currents and Generated Heat of the Adjacent Cable Over the Time, for Installation 1

Time (hour)	Current Phase a (A)	Current Phase b (A)	Current Phase c (A)	Current Phase n (A)	Heat of the adjacent cable (W/m)
0-1	0	0	0	0	0
1-2	200	100	50	132.28	4.8
2-3	400	200	300	173.20	76.8
3-4	50	400	200	304.13	19.2

TABLE S2
Conductor Currents and Generated Heat of the Adjacent Cable Over the Time, for Installation 1

Time (hour)	Current Phase a (A)	Current Phase b (A)	Current Phase c (A)	Current Phase n (A)	Heat of the adjacent cable (W/m)
0-1	0	0	0	0	0
1-2	400	0	0	400	76.8
2-3	0	500	100	458.25	76.8
3-4	0	100	400	360.55	76.8

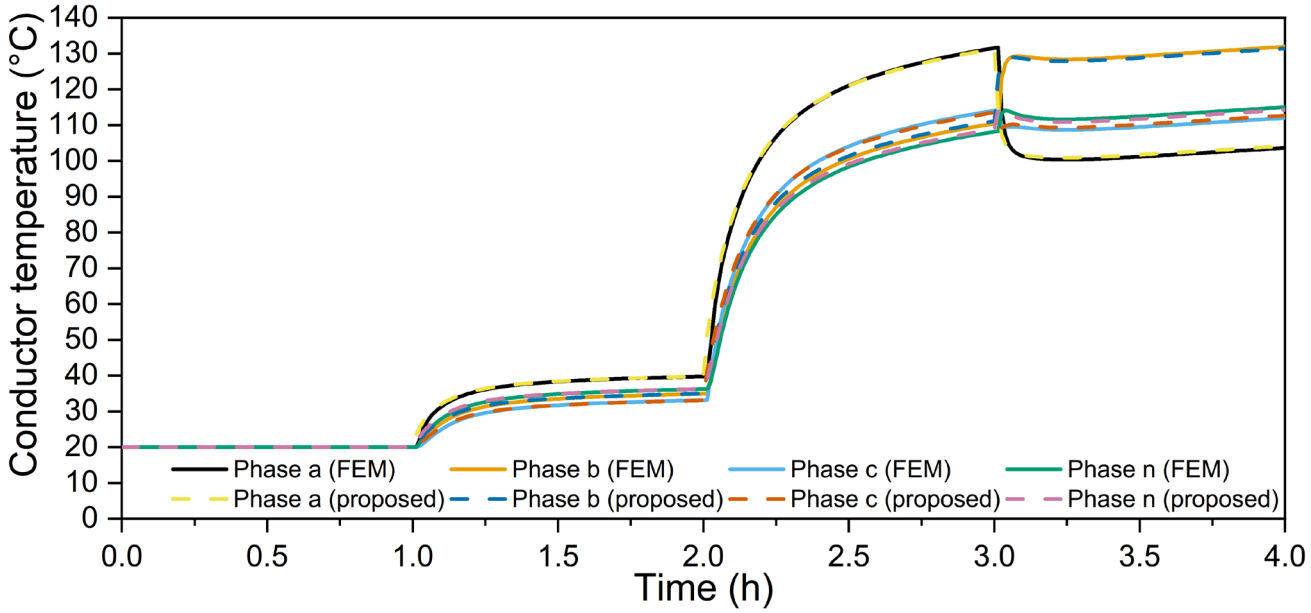

Fig. S1. Conductor temperatures for the input currents of Table S1 and underground *Installation 1*.

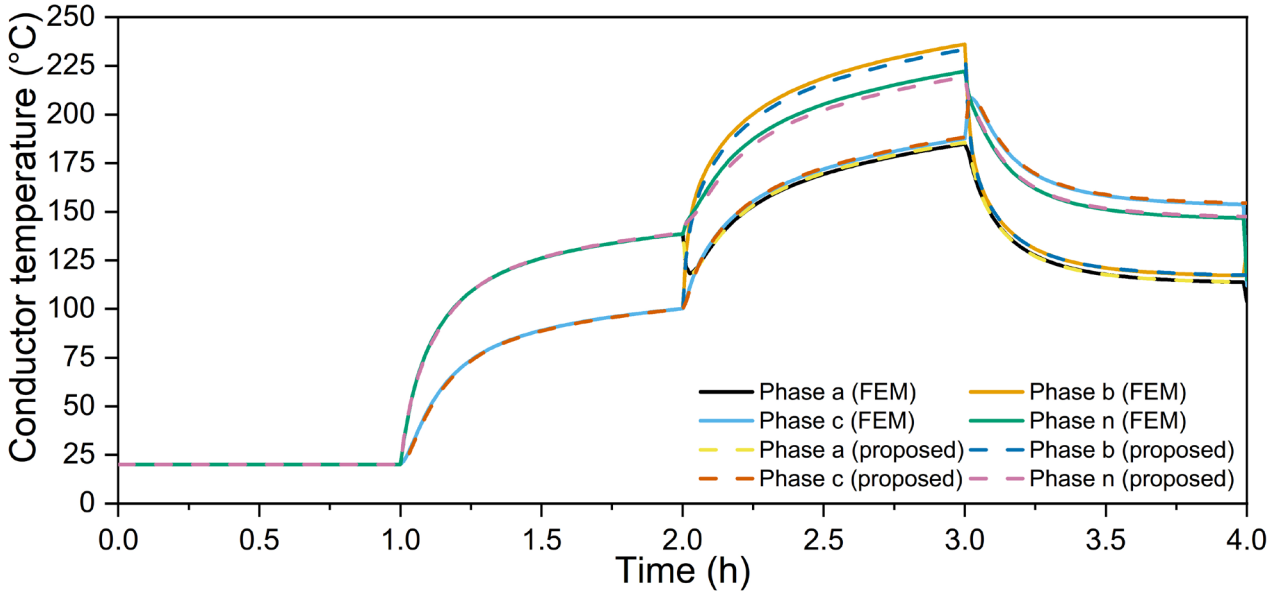

Fig. S2. Conductor temperatures for the input currents of Table S2 and underground *Installation 1*.

II. Consideration of Thermal Parameters Between the Diagonal Cores of 4-core Cables

In the TEE circuit of the manuscript, we neglected the diagonal thermal parameters between the diagonal conductors (a-c and b-n) of 4-core cables. Based on the simulation results of the investigated topologies, the neglect of diagonal thermal parameters affects only negligibly the accuracy of the TEE circuit. The extended TEE circuit with the inclusion of the diagonal parameters is depicted in Fig. S3 below. As shown, one additional thermal capacitor (C_d) and four additional thermal resistances (R_d) have been included in the proposed TEE circuit that connect the diagonal conductors.

In case that the diagonal thermal parameters are considered, the thermal resistances R_m and R_d should be calculated, as follows:

Calculation of diagonal resistance R_d: We load the conductors a, b, c in a FEM software so that they acquire the same temperature and no heat is flown through the resistances R_m. The heat produced by the conductor b is given by eq. (S1), as follows:

$$Q_b = \frac{T^b_{con} - T_d}{R_d} + \frac{T^b_{con} - T_{sur\_cab}}{3 \cdot R_s} \tag{S1}$$

where $Q_b, T^b_{con}, T_{sur\_cab}$ have all defined in the manuscript. T_d is the temperature measured by FEM at the center of the cable, namely at the diagonal capacitance C_d of Fig. S3.

Calculation of mutual resistance Rm: The mutual resistance R_m is calculated by eq. (S2), as follows:

$$Q_b = \frac{T^b_{con} - T^a_{con}}{2 \cdot R_m} + \frac{T^b_{con} - T^c_{con}}{2 \cdot R_m} + \frac{T^b_{con} - T_d}{R_d} + \frac{T^b_{con} - T_{sur\_cab}}{3 \cdot R_s} \tag{S2}$$

where the only unknown variable is R_m. Note that R_d has been calculated by eq. (S1) above, while the calculation of R_s has been explained in the manuscript.

It is clarified that when the diagonal parameters are considered, the resistance R_m is calculated by (S2), while when neglected, it is calculated by eq. (11) of the manuscript. As shown, one additional term is included in (S2) (namely $\frac{T^b_{con} - T_d}{R_d}$) that accounts for the R_d resistance. As a result, the R_m resistance of the extended TEE circuit of Fig. S1 takes a higher value compared with Fig 2 of the manuscript. In this respect, we can deduce that the diagonal elements have been indirectly considered in Fig. 2 of the manuscript, through the reduction of the R_m value.

The temperature responses of the TEE circuit without and with the diagonal elements are quoted in Figs S4 and S5, respectively. As shown, both circuits have excellent accuracy since their responses coincide almost completely with FEM. The maximum deviation between TEE and FEM for Figs. S4 and S5 at the peak is around 0.5 °C and 0.3 °C, respectively, indicating the negligible influence of diagonal elements.

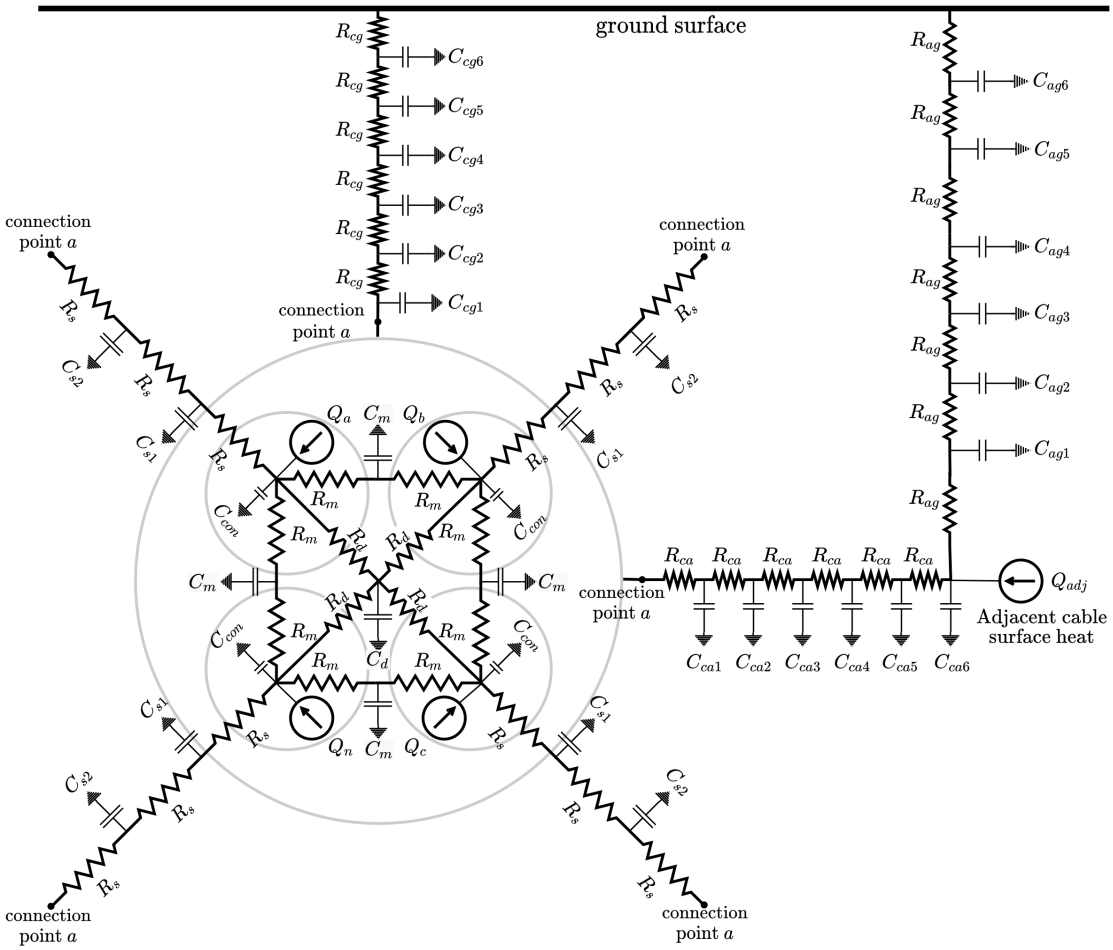

Fig. S3. Extended TEE circuit model of a 4-core underground cable considering also the diagonal elements between the diagonal cores (R_d, C_d).

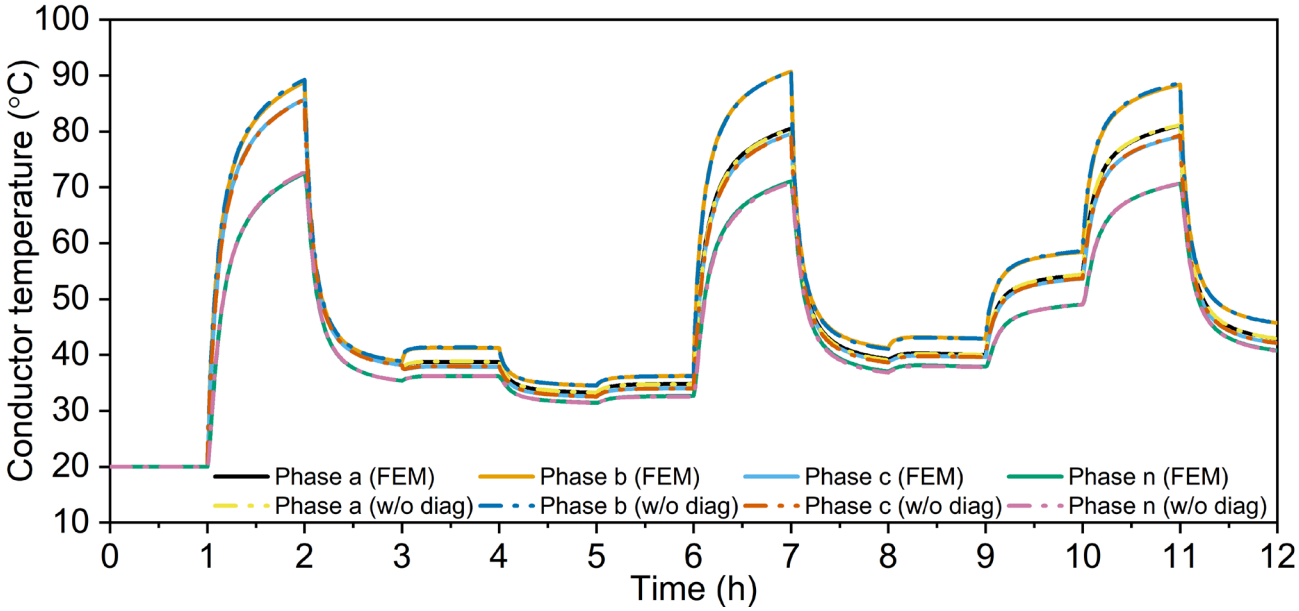

Fig. S4. Conductor temperatures for the input currents of Table 1 and underground *Installation 1*. The TEE circuit of Fig. 2 was applied without the diagonal elements.

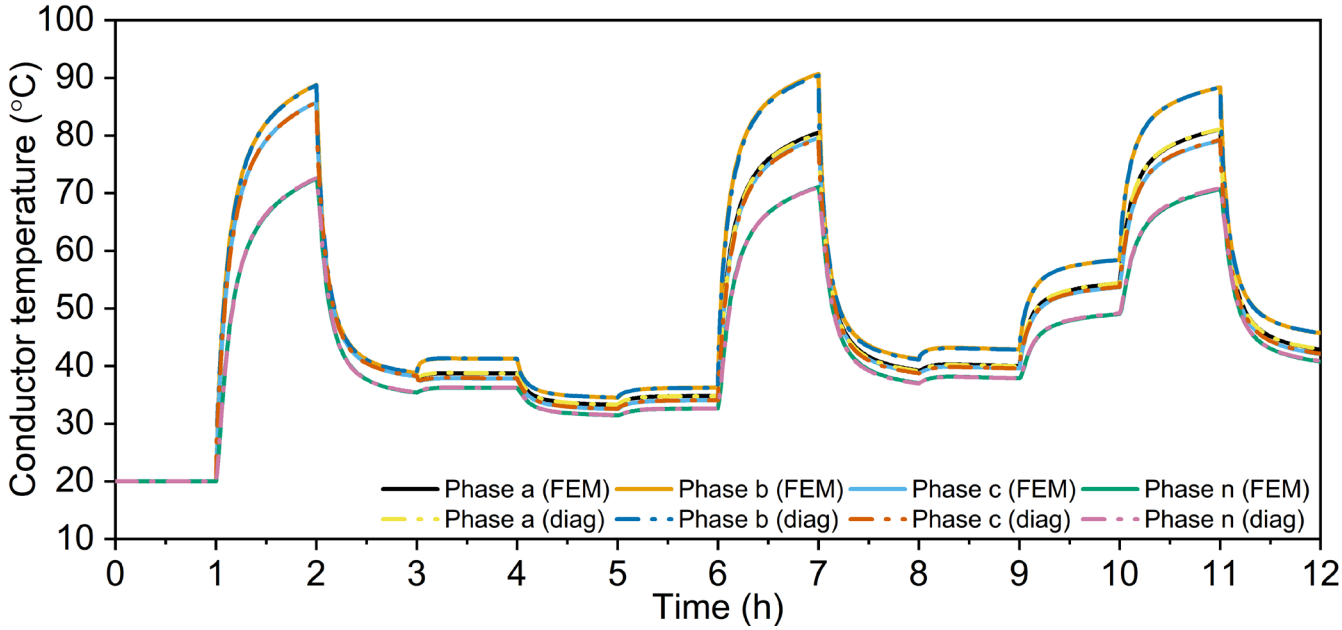

Fig. S5. Conductor temperatures for the input currents of Table 1 and underground *Installation 1*. The TEE circuit of Fig. S3 was applied with the diagonal elements.